

Performance Analysis of 3-D DWT, 3-D DFT, 3-D DCT, 3-D DHT for Medical Image Compression

Zain Ul Abidin

Department of Electrical Engineering,
University of Engineering & Technology Taxila – Pakistan

Gulistan Raja

Department of Electrical Engineering,
University of Engineering & Technology Taxila – Pakistan

Muhammad Haroon Yousaf

Department of Computer Engineering
University of Engineering & Technology Taxila – Pakistan

Abstract

Medical images have been widely in use for the diagnosis of different diseases. To deal with the huge storage requirements for these images, medical images compression has been one of the promising areas of research in last decade. This paper aims to analyze the performance of 3-D discrete wavelet transform (DWT), 3-D discrete cosine transform (DCT), 3-D discrete Hartley transform (DHT) and 3-D discrete Fourier transform (DFT) for the compression of medical images. Various MRI images and x-ray angiograms have been used for the implementation of these transforms. Medical images are divided into $8 \times 8 \times M$ block sizes, where M is the number of slices. 3-D transformed output coefficients are then quantized and encoded. Proposed research work evaluates the performance of these transforms on parameters like peak signal to noise ratio (PSNR), structural similarity index matrices (SSIM), bit error rate (BER) and Compression ratio (CR). Experimentation results have shown that for MRI images Daubechies wavelets gave highest performance than biorthogonal and Symlet wavelets; for Angiograms biorthogonal wavelets is found to be the most suitable. Experimentation results also indicates that 3-D DHT yields best PSNR values for MRI images and 3-D DCT is most suitable transform for the compression of angiographic images.

Key Words—Medical Image Compression, Discrete Cosine transform, Discret Fourier transform, Discrete Hartley transform, Discrete Wavelet transform.

I. INTRODUCTION

With the ever growing need of bandwidth and its scarcity, there is always a need to store and transmit information in a manner which requires minimum storage space and fast transmission rate. These days, medical images are one of the important sources of information used to diagnose patient ailment. For the patients residing at far locations these images are transferred to doctors through internet to diagnose and treat patient. Medical image compression has gained much attention as it allows fast transmission of medical images and requires low storage space while maintaining relevant diagnostic information. Different compression techniques are used for this purpose. These compression techniques can be categorized into two types. Lossy compression and lossless compression. Lossless compression techniques are usually used for compression of medical images. As the name indicates no information is lost in case of lossless compression. For medical images lossy compression is tolerable if it does not affect the diagnostic results [1].

3-D medical image compression is very important because most of the diagnosis carried out uses MRI, CT, PET, angiogram and other modalities. These modalities generate multiple slices of a single organ under examination [2]. Progressive variation of object in multiple 2-D slices placed one after another is visualized as 3-D imaging or it is the time sequence of slice images of dynamic object [3].

General block diagrams of compression and decompression are shown in fig. 1 and fig. 2 respectively.

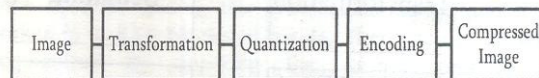


Fig. 1. Compression of an Image [4]

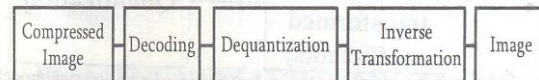


Fig. 2. Decompression of an Image [4]

To achieve compression input image data is first de-correlated by applying transformation. This transformed data is quantized and encoding is performed. Various linear transformation techniques have been developed, each transform has its benefits and draw backs. Human eyes are less sensitive to the higher frequencies hence higher components can be neglected without any apparent loss [5]. Medical image compression is more critical than compression for any other image. To avoid any unwanted situation special attention must be provided in this regard. Suitable choice of transform is very mandatory to achieve the desired goals i.e. High compression ratio and better PSNR maintaining correct diagnostic information.

For image compression in JPEG, DCT is used. Recently for image compression wavelet based transforms are used because even at higher compression rates the image quality is excellent [6]. Fortunately many wavelet filters exists each having different characteristics, for good coding performance selection of correct wavelet filter is very important [7].

This research work targets the implementation of 3-D DCT, 3-D DHT, 3-D DFT, 3-D Daubechies wavelet transform, 3-D Symlet transform and 3-D biorthogonal transform in order to find the most suitable transform and investigate the behavior of different wavelet filters for compression of different medical images. Transforms are applied on different medical images like MRI of abdomen, kidney, cardiac, brain, angiograms of liver and chest for compression purpose. Their performances are

compared on the basis of performance parameters like PSNR, SSIM. Bit rate and compression ratio[8].

II. PROPOSED METHODOLOGY

The block diagram of the implemented compression method is given in fig.3

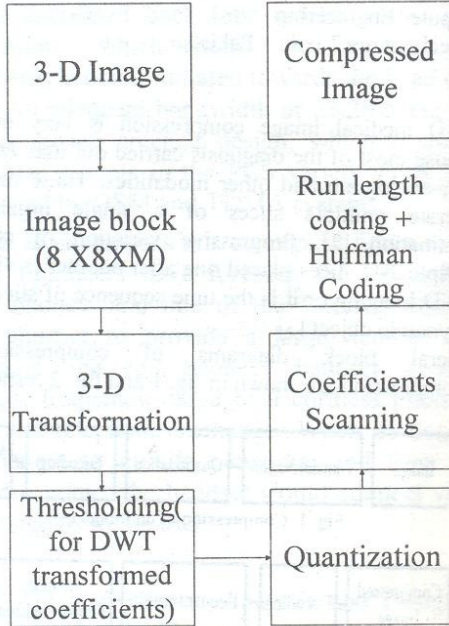


Fig. 3. Block diagram of proposed compression model

In the first step the 3-D medical image is split into 3-D data block of 8X8XM sizes. Number of slices considered are M=2, 4, 8 and 16. 3-D transformation is applied to block data to remove inter slice redundancy. Each 3-D transform is explained in the subsequent sections.

A. 3-D DHT:

For Hartley transform, 3-D DHT and 3-D inverse DHT are defined as given in equation (1) and (2) respectively [9].

$$P(\alpha, \beta, \gamma) =$$

$$\sum_{X=0}^{N_1-1} \sum_{Y=0}^{N_2-1} \sum_{Z=0}^{N_3-1} p(X, Y, Z) \text{Cas}\left(\frac{2\pi X\alpha}{N_1} + \frac{2\pi Y\beta}{N_2} + \frac{2\pi Z\gamma}{N_3}\right) \dots (1)$$

$$p(X, Y, Z) =$$

$$\frac{1}{N_1 N_2 N_3} \sum_{\alpha=0}^{N_1-1} \sum_{\beta=0}^{N_2-1} \sum_{\gamma=0}^{N_3-1} P(\alpha, \beta, \gamma) \text{cas}\left(\frac{2\pi X\alpha}{N_1} + \frac{2\pi Y\beta}{N_2} + \frac{2\pi Z\gamma}{N_3}\right) \dots (2)$$

Where $p(X, Y, Z)$ = original input voxel value.

$$\text{cas}(x) = \cos(x) + \sin(x),$$

$P(\alpha, \beta, \gamma)$ is the transformed voxel value.

In 3-D DHT the frequency harmonics increases towards centre within a slice and towards middle slice among different slices.

B. 3-D DCT and 3-D DFT:

Similarly 3-D DCT and 3-D DFT are implemented. In case of 3-D DCT only real part of 3-D DFT is considered that is cosine part only, imaginary part of discrete Fourier transform can be cancelled by replicating the real part. Whereas frequency harmonics in case of 3-D DCT and 3-D DFT increases from left to right and top to bottom within a slice and increases from first slice to last slice among different slices [4].

C. 3-D DWT:

Wavelet transform decomposes the signal into many smooth and detailed signals at multiple resolution level [10]. It can be implemented by using 2 channel filter bank [11]. In filter bank analysis filters and synthesis filters are connected by sampling operators. Wavelet transform is achieved by repetitively applying filter bank.

3-D wavelet transformation creates a number of blocks from the image set which have different level of energy. Among them, one block contains most of the energy and rests have other frequency band energy. One level implementation of 3-D wavelet transform is given in fig.4[12].

Daubechies (DB4), bi-orthogonal and Symlet wavelet filters are applied on the image data set [13]. For better coding performance filter order is very important. Filter coefficients are determined empirically. Three level of wavelet decomposition is employed.

In the first step by using low pass and high pass filters rows of an $N \times N$ are filtered. Convolution of filtered image with filters is applied in the second step results in four decomposed sub-volumes and produced sub image of size $(N/2) \times (N/2)$. Along the z-direction these four sub bands are filtered and generate eight sub volumes.

Wavelet transformed data consists of one low resolution component and many high frequency components. High frequency components contain less amount of energy as these components have less amplitude. So these components can be eliminated. A threshold value is chosen and amplitude value less than the threshold value is set to zero.

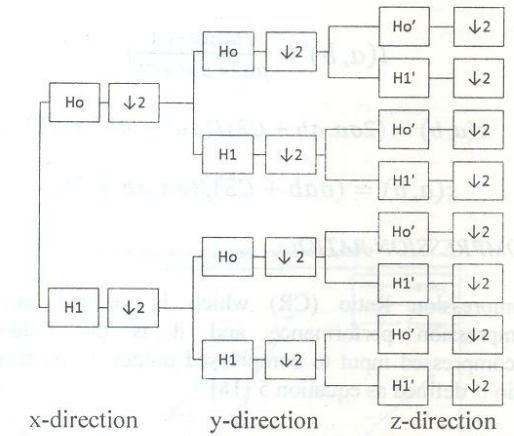


Fig. 4. One level implementation of 3-D wavelet transform[12]

Most of the energy lies in few transformed coefficients and remaining coefficients can be coarsely quantized or even set to zero. Quantization is a non linear process as it is many to few mapping hence it is lossy process. First 2-D quantization matrix is obtained empirically corresponding to first slice of the medical images using different test images so that the PSNR is more than 40 dB with minimum bit rate value. 3-D quantization matrix is obtained by using 2-D matrix as a basis and performing tests on various images keeping the same criteria of PSNR and bit rate value.

In case of 3-D DCT and 3-DFT Zigzag scanning is performed on individual slices sequentially shown in table.I. Whereas in case of 3-D DHT,2-D scanning used for the transformed coefficients is shown below in table II. On 3-D DWT quantized coefficients for all low pass subbands zigzag scanning is performed, for vertical subbands column scanning, for horizontal subbands row scanning and for diagonal subbands zigzag scanning is performed, it is shown in table III. Scanning order is indicated by the number the location.

TABLE I.2-D Scanning of DFT and DCT coefficients

1	2	6	7	15	16	28	29
3	5	8	14	17	27	30	43
4	9	13	18	26	31	42	44
10	12	19	25	32	41	45	54
11	20	24	33	40	46	53	55
21	23	34	39	47	52	56	61
22	35	38	48	51	57	60	62
36	37	49	50	58	59	63	64

TABLE II.2-D Scanning of DHT coefficients

1	5	13	25	40	24	12	4
6	14	26	41	52	39	23	11
15	27	42	53	60	51	38	22
28	43	54	61	64	59	50	37
29	44	55	62	63	58	49	36
16	30	45	56	57	48	35	21
7	17	31	46	47	34	20	10
2	8	18	32	33	19	9	3

TABLE III. 2-D Scanning of DWT coefficients

1	2	5	8	17	24	25	32
3	4	6	7	18	23	26	31
9	10	13	14	19	22	27	30
12	11	15	16	20	21	28	29
33	34	35	36	49	50	54	55
40	39	38	37	51	53	56	61
41	42	43	44	52	57	60	62
48	47	46	45	58	59	63	64

Run length coding is applied to the quantized data. RLC reduces the spatial redundancies and achieves compression. In RLC, row by row scanning of image takes place and values of the pixel are replaced by (run lengths, pixel values).After applying RLC, Huffman coding is applied to achieve further compression. In this coding scheme shorter bits are assigned to more probable pixel values and longer bits to less probable pixel values [14].

For decompression purpose decoding process was done by first loading the compressed image and then broken in to 8X8 blocks of pixels. Then each block was dequantized by applying the reverse process of quantization. Then each restored block is filtered through inverse transform and all blocks are combined to get the output image.

III. EXPERIMENTATION RESULTS AND DISCUSSION

Standard DICOM medical images [15] of six different organs were used for the performance evaluation of the 3D transforms and Wavelets. Different types of images were considered for experimental setup. The experimental data set used can be tabulated as table IV.

TABLE IV. Characteristics of DICOM Sample Images

Type of Image (Modality)	Resolution 3D (X*Y*M) M=No of Slices	Voxel Value Range
Brain MRI	256 X 256 X 16	0 to 255
Cardiac MRI	256 X 256 X 16	0 to 255
Knee MRI	256 X 256 X 16	0 to 255
Chest Angiography	512 X 512 X 16	0 to 255
Liver Angiography	512 X 512 X 16	0 to 255
Abdomen MRI	512 X 512 X 16	0 to 255

To illustrate the performance of each transform and wavelet, the designed code was simulated for different number of frames. For illustration, 16 frames for Brain MRI are shown in Fig. 5.

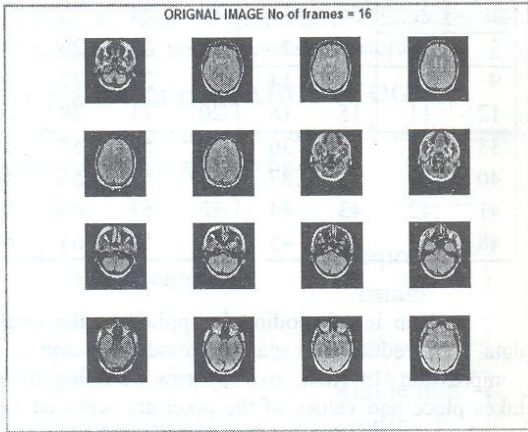


Fig. 5. 16 input frames for Brain MRI

Performance of the implemented compression techniques is evaluated in terms of three performance parameters i.e. PSNR, SSIM and CR. [8,16].

PSNR:

PSNR expresses the error between original information and reconstructed image after processing, which is considered as a general parameter for quality assessment and is generally applied in digital image processing. PSNR is calculated using equation 3[17]:

$$PSNR(dB) = \frac{20 \log_{10}(\text{Maximum voxel value})}{\sqrt{\frac{\sum_i \sum_j \sum_k (f(i,j,k) - F(i,j,k))^2}{N}}} \dots (3)$$

Where voxel value of reconstructed image is $F(i,j,k)$ at point (i, j, k) , N is the total number of voxel and $f(i, j, k)$ is the original input value at (i,j,k)

SSIM:

SSIM is another important metric of measurement of image quality. SSIM is a method to find the similarity between two images. To improve performance methods like MSE and PSNR, SSIM is designed because these method maybe are inappropriate with the human visual perception. SSIM factor is the average of the combined values of luminance, variance and structure. It measures the change in these three characteristics of two images let suppose "a" and "b". Average pixel intensity is represented as luminance $l(a,b)$, variance between the original and compressed image is defined as contrast, $c(a,b)$ and cross correlation between the original and compressed image by structure $s(a,b)$. SSIM between two images can have maximum value of "1" which indicates there is complete similarity between the images. The SSIM is defined in equations 4[17].

$$SSIM(a, b) = l(a, b)c(a, b)s(a, b) \dots \dots \dots (4)$$

Where

$$l(a, b) = \frac{2\mu_a\mu_b + C1}{\mu_a^2 + \mu_b^2 + C1}$$

$$c(a, b) = (2\sigma_a.\sigma_b + C2)/(\sigma_a^2 + \sigma_b^2 + C2)$$

$$s(a, b) = (\sigma_{ab} + C3)/(\sigma_a.\sigma_b + C3)$$

COMPRESSION RATIO:

Compression Ratio (CR) which is defined as the compression performance and it is the ratio of uncompressed input to compressed output. Compression ratio is defined as equation 5 [18].

$$CR = \frac{\text{original bits per voxel}}{\text{Compressed bits per voxel}} \dots \dots \dots (5)$$

Figure 6 shows the original image for Brain MRI for 8 numbers of frames and output for Hartley, Cosine and Fourier transform.

A. Brain MRI Results for PSNR vs Bitrate

For $M=8$, the behavior of different transforms for the Brain MRI images is shown in fig 6.

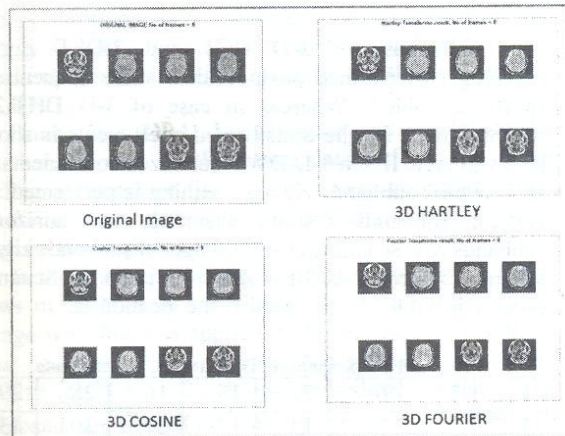


Fig. 6. Original and output images of Brain MRI for Transforms

PSNR graphs for different number of frames i.e 2, 4, 8, 16 for the 3D Hartley, cosine and Fourier transforms are also shown in figure 7(a), figure 7(b), and figure 7(c) and figure 7(d). The Hartley has proven to be more efficient in term of PSNR than other transforms for both low and higher bitrates which is very obvious form the values given in table II and shown in figures 8(a), 8(b) and 8 (c).

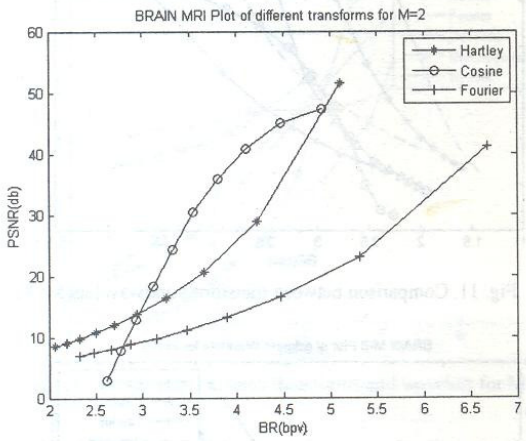


Fig. 7(a). PSNR vsbpv graphs for transforms (M=2)

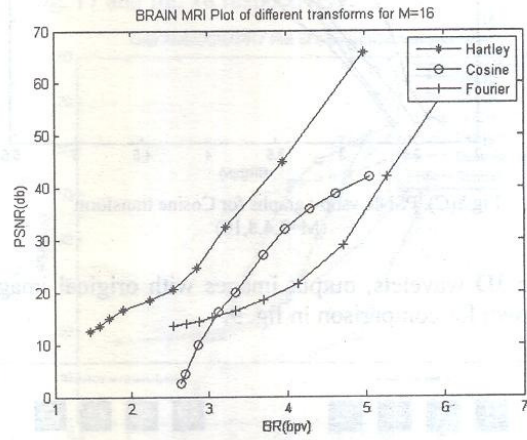


Fig. 7(d). PSNR vsbpv graphs for transforms (M=16)

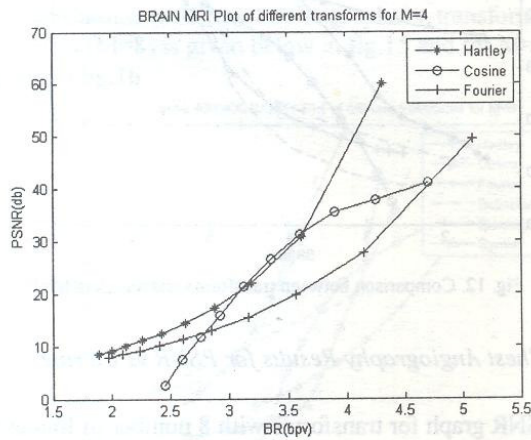


Fig. 7(b). PSNR vsbpv graphs for transforms (M=4)

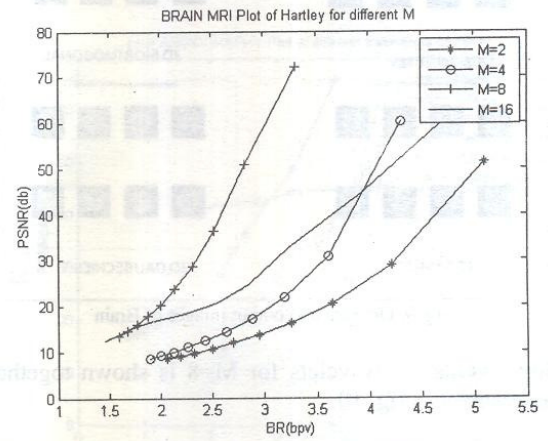


Fig. 8(a). PSNR vsbpv graphs for Hartley transform (M=2,4,8,16)

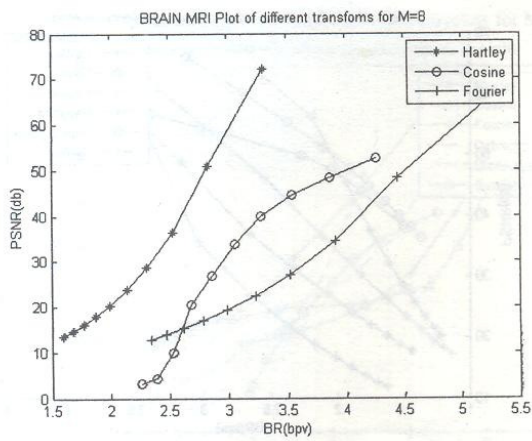


Fig. 7(c). PSNR vsbpv graphs for transforms (M=8)

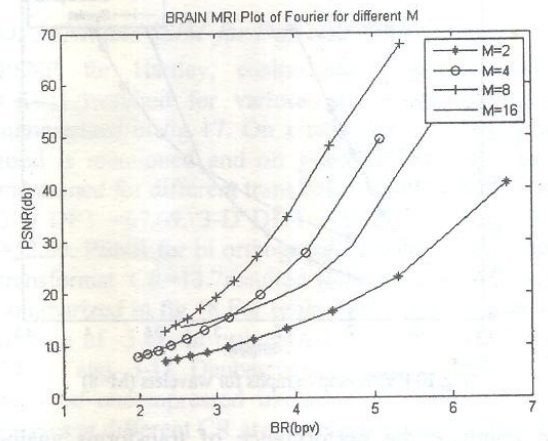


Fig. 8(b). PSNR vsbpv graphs for Fourier transform (M=2,4,8,16)

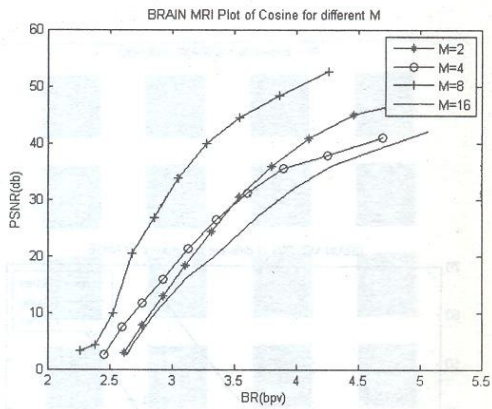


Fig.8(C). PSNR vsbpv graphs for Cosine transform (M=2,4,8,16)

For 3D wavelets, output images with original image are shown for comparison in fig. 9.

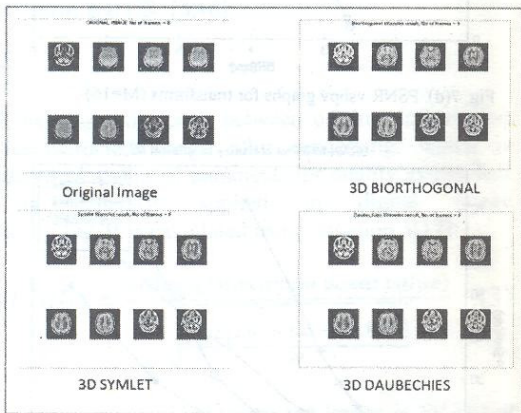


Fig. 9. Original and output images of Brain

Now results for wavelets for M=8 is shown together for assessment in fig. 10.

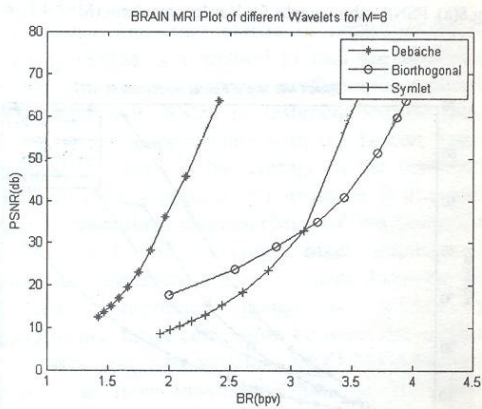


Fig.10 PSNRvsbpv graphs for wavelets (M=8)

To compare the performance of transforms against wavelets, PSNR values for both transforms and wavelets

are plotted together in the fig. 11 and fig. 12 respectively for M=8 and M=16.

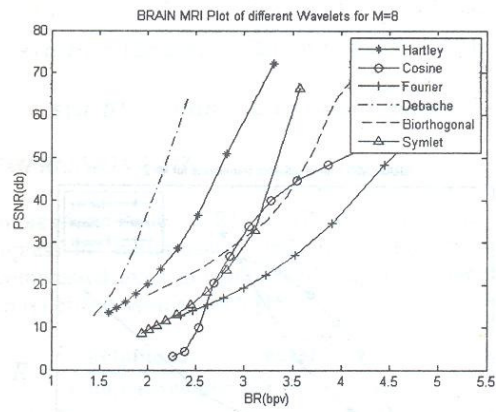


Fig. 11. Comparison between transforms and wavelets(M=8)

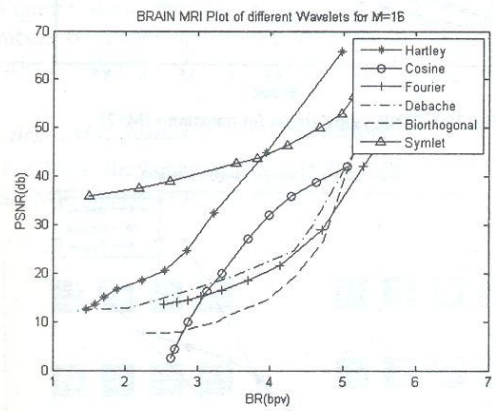


Fig. 12. Comparison between transforms and wavelets(M=16)

B. Chest Angiography Results for PSNR vs Bit rate

PSNR graph for transforms with 8 number of frames is shown in fig. 13 and PSNR graph with 16 number of frames is shown in fig.14 respectively.

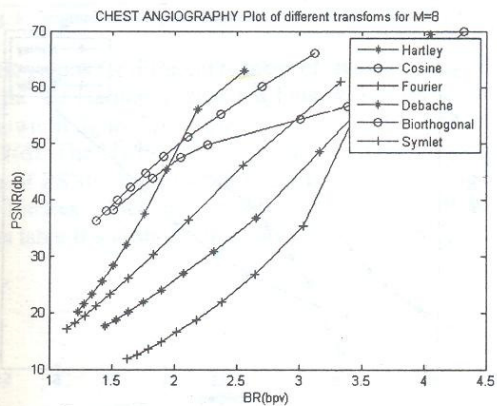


Fig. 13. Comparison between transforms and wavelets for M=8

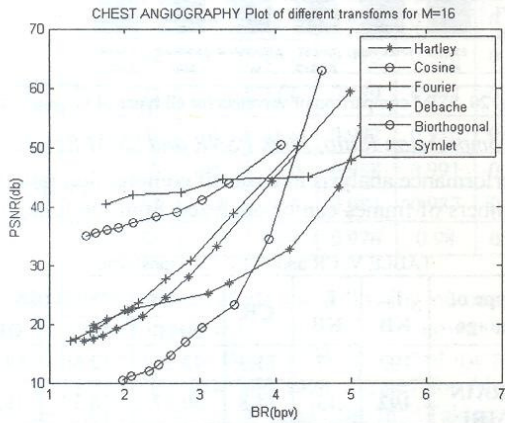


Fig. 14. Comparison between transforms and wavelets for M=16

C. Cardiac MRI and Liver Angiography Results for PSNR vs Bitrate

For Cardiac MRI, the PSNR graph for transforms and wavelets (M=8) is given below in fig.15 and for M=16 is given in fig.16 .

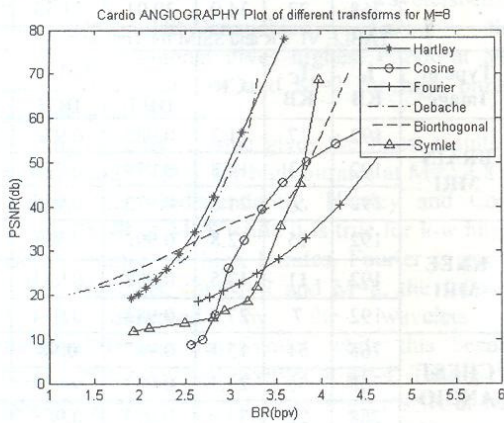


Fig. 15. Comparison between transforms and wavelets for M=8

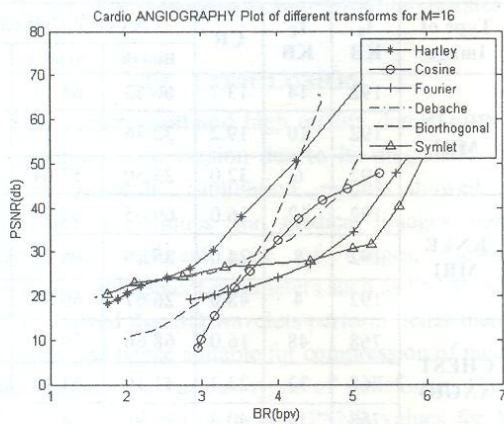


Fig. 16. Comparison between transforms and wavelets for M=16

For Liver angiogram, the PSNR graph for transforms and wavelets for M=8 and for M=16 is given below in fig. 17 and fig. 18 respectively.

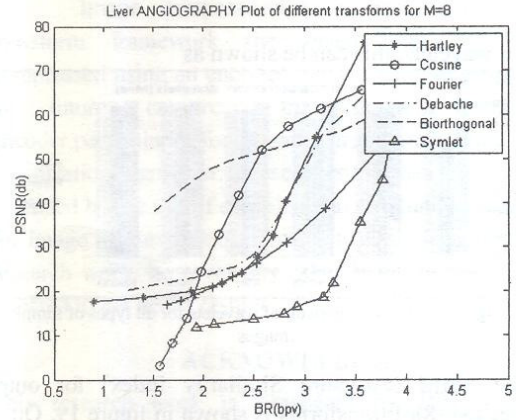


Fig. 17. Comparison between transforms and wavelets for M=8

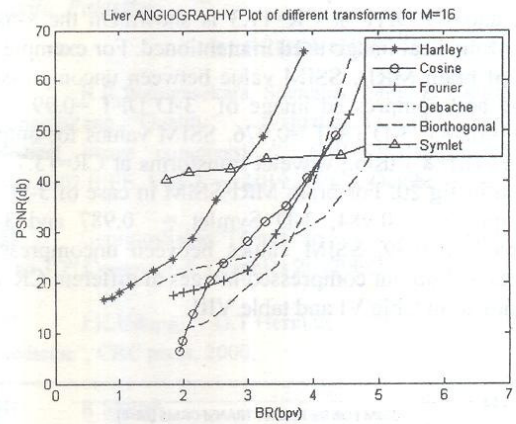


Fig. 18. Comparison between transforms and wavelets for M=16

D. PSNR and SSIM for Different Type of Images

PSNR for Hartley, cosine and Fourier transform CR=11.3 resulted for various set of images (M=8) is summarized in fig 17. On x-axis type of medical image used is mentioned and on y-axis PSNR (dB) value is mentioned for different transforms. PSNR value in case of 3-D DFT =67.69, 3-D DHT =72.25 and for 3-D DCT =52.60. PSNR for bi orthogonal, Symlet and Daubechies transform CR=13.7 resulted for various set of images is summarized in fig 18. For brain MRI image PSNR values in case of 3-D bi orthogonal = 66.43, 3-D Symlet = 65.11 and 3-D Daubechies =71.65 . PSNR values between uncompressed images and output compressed images at different CR are mentioned in table V and table VII.

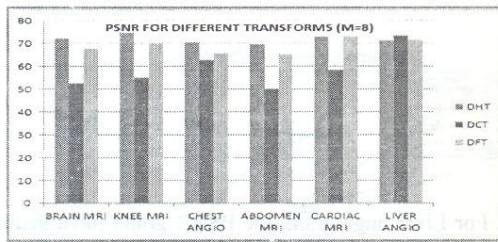


Fig. 17. PSNR comparison of transforms for all types of sample images

For wavelets, this can be shown as

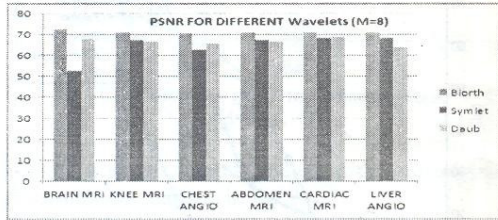


Fig. 18. PSNR comparison of wavelets for all types of sample images

The SSIM (Structure Similarity Index) for output images ($M=8$) of transforms is shown in figure 19. On y-axis SSIM value between the uncompressed original image and output compressed image using 3-D DCT, 3-D DFT and 3-D DHT at $CR=11.3$ is shown. On the x-axis type of medical image used in mentioned. For example in case of brain MRI, SSIM value between uncompressed image and compressed image of 3-D DFT = 0.99, 3-D DHT = 0.983, 3-D DCT = 0.976. SSIM values for output images ($M=8$) using wavelet transforms at $CR=13.7$ are shown in fig 20. For brain MRI SSIM in case of 3-D bi orthogonal = 0.984, 3-D Symlet = 0.987 and 3-D Daubachies = 0.99. SSIM values between uncompressed images and output compressed images at different CR are mentioned in table VI and table VIII.

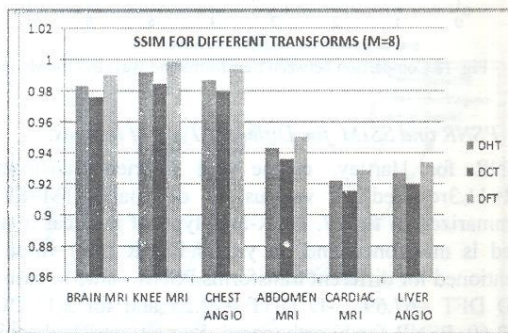


Fig. 19. SSIM comparison of transforms for all types of sample images

For output images from wavelets, SSIM results are

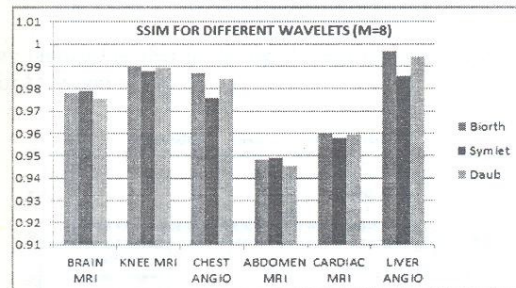


Fig. 20. SSIM comparison of wavelets for all types of sample images

E. Compression Ratio, Peak PSNR and SSIM Results

Performance analysis in terms of compression ratio for 8 numbers of frames can be analyzed from the following tables.

TABLE V. CR and PSNR for Transforms

Type of Image	I_0 KB	I_c KB	CR	AVG PSNR (dB)		
				DHT	DCT	DFT
BRAIN MRI	192	17	11.3	72.25	52.60	67.69
	192	13	14.8	50.97	48.37	48.22
	192	9	21.3	36.45	44.52	34.59
KNEE MRI	192	15	12.8	69.32	65.96	61.05
	192	11	17.5	48.54	60.05	45.97
	192	7	27.4	36.82	55.14	36.45
CHEST ANGIO	768	51	15.1	70.45	62.85	65.76
	768	36	21.3	54.27	57.71	46.90
	768	22	34.9	39.01	51.33	33.98

TABLE VI. CR and SSIM for Transforms

Type of Image	I_0 KB	I_c KB	CR	SSIM		
				DHT	DCT	DFT
BRAIN MRI	192	17	11.3	0.983	0.976	0.990
	192	13	14.8	0.979	0.972	0.986
	192	9	21.3	0.973	0.966	0.980
KNEE MRI	192	15	12.8	0.992	0.985	0.999
	192	11	17.5	0.988	0.981	0.995
	192	7	27.4	0.981	0.974	0.988
CHEST ANGIO	768	51	15.1	0.987	0.98	0.994
	768	36	21.3	0.983	0.976	0.990
	768	22	34.9	0.975	0.968	0.982

TABLE VII. CR and PSNR for Wavelets

Type of Image	I_0 KB	I_c KB	CR	AVG PSNR (dB)		
				Biorth	Symlet	DEB
BRAIN MRI	192	14	13.7	66.43	65.11	71.65
	192	10	19.2	32.76	61.30	50.67
	192	6	32.0	23.50	57.64	36.13
KNEE MRI	192	12	16.0	69.65	69.99	68.89
	192	8	24.0	35.29	66.25	56.08
	192	4	48.0	26.67	60.95	45.54
CHEST ANGIO	768	48	16.0	68.66	70.82	74.56
	768	33	23.3	41.10	61.43	55.12
	768	19	40.4	29.96	54.55	41.01

TABLE VIII. CR and SSIM for Wavelets

Type of Image	I ₀ KB	I _C KB	CR	SSIM		
				Biorth	Symlet	DEB
BRAIN MRI	192	14	13.7	0.984	0.987	0.990
	192	10	19.2	0.980	0.983	0.986
	192	6	32.0	0.974	0.977	0.980
KNEE MRI	192	12	16.0	0.993	0.996	0.999
	192	8	24.0	0.989	0.993	0.995
	192	4	48.0	0.982	0.986	0.988
CHEST ANGIO	768	48	16.0	0.988	0.991	0.994
	768	33	23.3	0.984	0.987	0.990
	768	19	40.4	0.976	0.98	0.982

Simulation results conclude the following outcomes for the 3D transforms and Wavelets as shown by the simulation results. For Brain MRI, in case of transforms, Cosine is best for low and high bitrates for M=2 and Hartley for M=4, M=8 and M=16. Taking them individually concludes that Cosine and Fourier gives highest PSNR for both low and high bitrates when M=8, and the same for Hartley for low bitrates. For High bitrates, Hartley performs best at M=16.

For M=2, the wavelets follow the high PSNR to low PSNR as biorthogonal>Debauchies>Symlet while this becomes Debauchies>Biorthogonal>Symlet for M=4. At M=8, wavelets behaves Biorthogonal>Symlet>Debauchies. Taking them separately, Biorthogonal gives highest PSNR at M=8, Symlet at M=16 for low and M=2 for high bitrates, Debauchies at M=4.

For Angiography, Cosine gives the finest results for low bitrates and Hartley for high bitrates at M=2,4,8 and 16. Taking them independently, Hartley and Cosine gives high PSNR at M=8 while it is true for low bitrates in case of Fourier. At high bitrates, Fourier is good at M=4. For Wavelets, for M=2 and M=8, the following order is observed by the wavelets i.e. Biorthogonal>Debauchies>Symlet while this becomes Debauchies>Biorthogonal>Symlet at M=4. Taking them independently, Biorthogonal gives high PSNR at M=8, Symlet at M=16 for low and M=2 for high bitrates and Debauchies at M=4 for low and M=2 for high bitrates.

IV. CONCLUSION

Low rate compression and high quality demands by the medical image compression due to its diagnostic value are very difficult. Simulation results showed that compression techniques for medical images behave different for different type of images. However, performance assessment parameters such as PSNR, SSIM and CR showed that 3D wavelets perform better than 3D transforms and hence suitable for compression of medical images. Among the various types of transforms, Hartley has been found to result in best PSNR values for MRI

images and results evaluate that Cosine is most suitable candidate for the compression of angiographic images. From different types of wavelets, Debauchies gave highest performance for MRI images than Biorthogonal and Symlet families of wavelets and highest results for PSNR were achieved by Biorthogonal wavelet for Angiography and thus suitable for these types of images.

Image compression is a vast subject. In a transform framework the image can be further compressed using an encoder. So, the next step would be to future compress the image using an encoder, particularly for wavelet transforms with better quantization algorithm. These possibilities can be further extended by the use of complex wavelet functions applied for image decomposition. Huffman was used during this research work, however any other better option may be selected to get better results.

ACKNOWLEDGE

This research work is supported by Directorate of Advance Studies, Research and Technological Development, University of Engineering and Technology Taxila, Pakistan.

REFERENCES

- [1] N.R.Wanigasekara, Shenghao Ding, Zhuangzhi Yan, YongqinZeng, "Quality evaluation for JPEG 2000 based medical image compression", EMBS/BMES Conference, Proc.2002 IEEE, Vol. 2, pp.1019 – 1020, October 2002
- [2] GeorgiosSakas "Trends in medical imaging: from 2D to 3D" Computers & Graphics 26 (2002) 577–587.
- [3] J.K.Udupa, G.T.Herman, "3-D Imaging in Medicine", CRC press, 2000.
- [4] R.Shyam Sunder, C.Eswaran, N.Sriramm, "Performance Evaluation of 3-D Transforms for Medical Image Compression" IEEE International Conference on Electro Information Technology, 2005.
- [5] Stephen.J.Solari, "Digital video and audio compression", McGraw-Hill 1997
- [6] B. Ramakrishnan and N. Sriraam, "Internet transmission of DICOM images with effective low bandwidth utilization", Digital Signal Processing, Vol. 16, pp. 825–831, 2006.
- [7] S. Udomhunsakul and K. Hamamoto, "Wavelet filters comparison for ultrasonic image compression," Conf. IEEE TENCON, vol. 1, Nov. 2004, pp. 171-174.

[8] Alain Hore, DjemelZiou. " Image quality metrics: PSNR vs. SSIM " International conference on pattern recognition,2010.

[9] Boussakta.S, Alshibami.O.H, Aziz.M.Y, "Radix-2 × 2 × 2 algorithm for the 3-D discrete Hartley transform", IEEE Trans. On Signal Processing, Vol. 49, Issue.12, pp3145 –3156, December 2001.

[10] Ruchika, Mooninder Singh, Anant Raj Singh,"Compression of Medical Images Using Wavelet Transforms" , International Journal of Soft Computing and Engineering (IJSCE) , May 2012.

[11] M. Vetterliand C. Herley, "Wavelets and filter banks: Theory and design" IEEE Trans. Signal Processing, vol. 40, pp. 2207-2232, 1992.

[12] Jun Wang , H. K. Huang,"Medical Image Compression by Using Three-Dimensional Wavelet Transformation"IEEETransactions on medical imaging, vol. 15, no. 4, August 1996.

[13] Bairagi, V.K. , "Selection of Wavelets for Medical Image Compression" in IEEE International Conference on Advances in computing, control and telecom technologies, 2009, India, pp 678-680.

[14] Lakhani, G, Lubbock, "Modified JPEG Huffman coding" IEEE Transactions on Image Processing, vol.12, no.2, Feb 2003.

[15] DICOM Test Medical Images available on-line at <http://medical.nema.org/medical/dicom/Multiframe/>, accessed June 2012.

[16] V.Bhaskaran, K.Konstantinides, "IMAGE AND VIDEO COMPRESSION STANDARDS Algorithms and Architectures", Kluwer Academic publishers 1996.

[17] Z.Wang, A.C.Bovik, H.R. Sheikh and E.P simoncelli, "Image quality assessment: from error visibility to structural similarity", IEEE transaction on image processing, vol.13.no.4, pp.600-612, 2004.

[18] Tzi-CkerChiueh, Chuan-Kai Yang, Taosong He, H.Pfister, A.Kaufman, "Integrated volume compression and visualization", Visualization '97, Proc. IEEE, pp 329 – 336, October 1997.

Quotation

➤ Education is helping the child realize his potentialities.

Erich Fromm

➤ Everyman believes that he has a greater possibility.

Ralph Waldo Emerson

➤ Nature is often hidden, sometimes overcome, seldom extinguished.

Francis Bacon

➤ Those who make the worst use of their time are the first to complain of its brevity.

Jean de La Bruyere

➤ Revolutions are the locomotives of history.

Nikita S. Khrushchev

➤ Revolution accelerates evolution

Kelly Miller

➤ When reform becomes impossible, revolution becomes imperative.

Kelly Miller

➤ Variety is the mother enjoyment.

Banjamin Dusraeli

➤ Money is like manure. If you spread it around, it does a lot of good, but if you pile it up in one place, it stinks like hell.

Clint W. Murchison

➤ Science may have found a cure for most evils; but it has found no remedy for the words of them all – the apathy of human beings.

Helen Keller

➤ If you want to lift yourself up, lift up someone else.

Booker T. Washington